

Niobium Electropolishing Using an HF-free Electrolyte

A. Lozano-Morales,* M. Inman and E.J. Taylor
Faraday Technology, Inc.,
Clayton, Ohio, USA

An alternative electrochemical process to chemical polishing and conventional electropolishing of niobium is discussed in this paper. The state-of-the-art in polishing technology uses either buffered chemical polishing with an electrolyte containing one part hydrofluoric (40%), one part nitric (65%), and two parts phosphoric (85%) acids by volume, or conventional electropolishing with an electrolyte containing 10% hydrofluoric (40%) and 90% sulfuric (96%) acids. Both processes use hydrofluoric acid, which is believed to be the only chemical capable of removing the natural inert film (Nb_2O_5) present on niobium. The pulse/pulse reverse process combines electrochemical waveform parameters, cell geometry, electrolyte and hydrodynamic conditions to control oxide film formation during electropolishing, eliminating the "environmental insult" associated with the use of hydrofluoric acid. With the new hydrofluoric acid-free polishing process, an average surface roughness down to $0.1\text{ }\mu\text{m}$ was obtained at an electropolishing rate of $5\text{ }\mu\text{m/min}$, which is five and ten times faster than buffered chemical polishing and conventional electropolishing, respectively.

Keywords: electropolishing, hydrofluoric acid-free, niobium, pulse/pulse reverse waveforms

Introduction

Niobium (Nb) is the current material of choice for the fabrication of superconducting radio frequency (SRF) accelerators due to its excellent superconducting properties. The performance of the accelerators is strongly dependent on the smoothness and cleanliness of the surface. The state-of-the-art in polishing technology for niobium superconducting cavities uses either chemical polishing or electropolishing.¹ In buffered chemical polishing, a mixture of concentrated nitric (HNO_3), hydrofluoric (HF) and phosphoric (H_3PO_4) acids is used. The nitric acid forms a niobium oxide layer, which is dissolved by the hydrofluoric acid, with the phosphoric acid acting as a buffer to prevent high reaction temperatures.² Typical removal rates achieved using this polishing technique are about $1\text{ }\mu\text{m/min}$. However, the resulting surface roughness is an order of magnitude higher than conventional electropolishing and the grain

boundaries are enhanced, which may degrade the quality factor.³ In conventional electropolishing, an electrolyte of concentrated sulfuric (H_2SO_4) and hydrofluoric (HF) acids is used in combination with a constant voltage that has to be adjusted with the changing temperature of the electrolyte. Conventional electropolishing achieves metal removal rates up to $0.5\text{ }\mu\text{m/min}$.^{1,4} Higher rates (e.g., $0.65\text{ }\mu\text{m/min}$) have been obtained with buffered electropolishing,³ which uses an electrolyte consisting of lactic, H_2SO_4 and HF acids. Conventional and buffered electropolishing techniques produce smoother surfaces than chemical polishing (e.g., R_a less than $0.1\text{ }\mu\text{m}$).

Other applications where HF is required for chemical and electrochemical polishing are for medical and dental implants made of niobium-alloys. Specifically, niobium and niobium alloys are hypoallergenic, and are typically the safest metals tolerated by the human body.⁵ Consequently, it is commonly alloyed with titanium and zirconium to make implantable metallic biomaterials for medical and surgical applications.^{6,7} Other metals and alloys of interest for medical/dental implants include titanium, titanium-molybdenum alloy and titanium-nickel. All of these materials require HF for polishing. According to Professor Lyle Zardiackas, former Chair of the Biomedical Materials Science Department at the School of Dentistry at University of Mississippi,⁸ elimination of HF for electrochemical polishing of medical/dental implants is an important need.

Disadvantages of both chemical and conventional electrochemical processes include the use of HF to achieve breakdown of the strong passive film on the surface, and possible incorporation of hydrogen into the substrate as a byproduct of the reactions. Ideally, a polishing process for SRF Nb cavities, surgical devices and metallic implants will have attributes that include the following:

* Corresponding author:
Alonso Lozano-Morales, Ph.D.
Faraday Technology, Inc.
315 Huls Drive
Clayton, OH 45315
Phone: (937) 836-7749
Fax: (937) 836-9498
Email: alonsolozano@faradaytechnology.com

- An electrolyte free of HF
- Control of average surface roughness (R_a) to a microscale finish, $R_a < 0.1 \mu\text{m}$
- Surface free from contamination after polishing
- Current distribution control that enables uniform polishing across the entire device
- Minimization of the absorption of hydrogen into the bulk material
- Controlled removal of at least $30 \mu\text{m}$ for medical implants⁹ (e.g., heart valve frames made from SS 316LVM) and $100 \mu\text{m}$ for SRF Nb cavities during polishing.

The conventional polishing processes described above have something in common. They all use HF, which is considered “an environmental insult.” It is believed that breakdown of the strong passive film on the niobium surface can be achieved only with the use of HF. In this paper, we describe how the Faradaic, or pulse/pulse reverse waveform electropolishing process controls oxide film formation during metal removal to achieve a microscale surface finish without the use of HF. The pulse/pulse reverse electropolishing process, described below, employs sophisticated electric fields to control oxide film formation during metal removal, eliminating the use of HF employed by conventional polishing techniques.

Pulse / pulse reverse HF-free electropolishing process

Although pulse/pulse reverse electropolishing is an electrochemical process, it stands apart from conventional electropolishing processes by the utilization of pulse/pulse reverse waveforms. Progress in conventional electrochemical engineering technology is hampered by a reliance on the art of chemical mediation for process control of advanced metal finishing technology at the expense of electrical and other physical parameter mediation. The reliance on chemical mediation art may be traced back 150 years, when the understanding of electrochemical principles was nascent. For example, the history of electrochemical processing is full of stories regarding the serendipitous discovery of chemical components of electrolytes leading to the desired surface properties.¹⁰ These discoveries ultimately became the paradigm for development of new electrolyte chemistries, which led to the proprietary chemical additives of today’s chemical suppliers. This chemical mediation paradigm has led to side effects of environmental waste and worker safety concerns, poor process control and process performance limitations. Consequently, electrochemical-polishing electrolytes can be complex, difficult to control and environmentally unfriendly.

By shifting the paradigm from chemical additives to the electrochemical science of kinetics and mass transport phenomena, we can utilize waveforms to develop an electrochemical surface finishing technology for advanced medical, semiconductor and aerospace materials and components. This pulse/pulse reverse approach will eliminate or reduce the need for HF in niobium finishing operations, as well as for other applications where HF is required for chemical and electrochemical polishing such as medical and dental implants. The pulse/pulse reverse process is environmentally benign and retains the advantages of high speed and low capital investment.

Much of the initial work on pulsed electrolysis has focused on plating processes.¹¹ However, pulse and pulse reverse electrolysis have recently been applied to special applications in edge and surface finishing.^{12,13} A generalized pulsed electrolysis waveform, including reverse pulse, is shown in Fig. 1. Pulsed electrolysis consists of an anodic peak current density, i_a , and associated on-time, t_a , a cathodic peak current density, i_c , and associated on-time, t_c , and an off-time, t_o . (**Please note: Voltage control is often preferred for metal removal; however, it is easier to discuss the theory in terms**

of current control.) The sum of the on- and off-times is the period of the waveform and the inverse of the period is the frequency. The anodic, D_a (or D_p), and cathodic, D_c (or D_r), duty cycles are the ratios of the respective on times to the period. The average current density, or net removal rate, i_{ave} , is given by:

$$i_{\text{avg}} = i_a \cdot D_a - i_c \cdot D_c \quad (1)$$

In contrast to conventional DC processes (e.g., electrochemical machining (ECM) and electropolishing (EP)) where the control variable is either constant voltage or current, the pulse/pulse reverse process introduces several key process parameters that are user defined:

- Peak anodic current density
- Anodic on-time
- Peak cathodic current density
- Cathodic on-time and
- Duty cycle.

The proper selection of these variables is critical for the successful implementation of the process, due to the strong influences that the variables have on mass transport rates, current distribution and metal removal rates.

Oxide film control for passive materials

Advanced materials form an oxide film that is self-healing and reforms in the presence of oxygen or even water. Since this passive film has low electrical conductivity and prevents the workpiece from a direct contact with the electrolyte, normal anodic dissolution cannot proceed without breakdown of the film. For conventional electrochemical polishing and non-steady state processing, high cell voltages and/or highly toxic acids such as HF are required to breakdown the oxide passive layer. Partial breakdown of the oxide film often occurs which causes pits on the surface. The proposed pulse/pulse reverse polishing process addresses this pitting

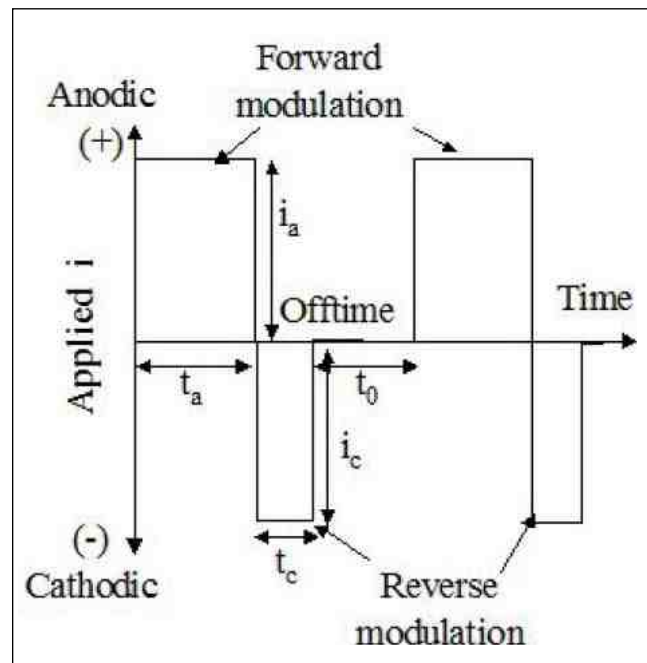
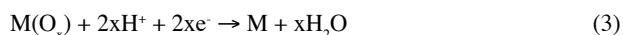


Figure 1—Generic pulse/pulse reverse waveform.

problem by reducing the passive film during the reverse period. By properly adjusting the process parameters, we can selectively consume the nascent oxygen gas or the oxide film on the workpiece by the following reactions:



Therefore, the pulse/pulse reverse process can reduce/eliminate the oxide film rehealing and eliminate the pits associated with partial oxide film breakdown.

Mass transport effects

The theory of mass transport during pulsed electrolysis has been discussed previously.^{14,15,16} In steady-state electrolysis (*i.e.*, constant current processes), the diffusion layer thickness, δ , is a time-invariant quantity for a given cell geometry and the solution hydrodynamic condition that develops within it. In pulsed electrolysis, δ begins to establish itself as soon as the electric field is applied. Therefore, the diffusion layer thickness is zero at the beginning of the pulse and gradually increases to its steady state value, which is what happens during a direct current process. In pulsed electrolysis, however, the current can be interrupted before δ is fully established. By selecting the appropriate subsequent off-time, this allows the dissolved ions to diffuse away from the electrode surface and allow the surface concentration to drift back to its original value before the next current interruption. Therefore, the concentration of reacting species in the vicinity of the electrode pulsates with the frequency of the modulation. The corresponding diffusion limiting current density, which is a measure of the removal rate, would be equal to an infinite value at time zero and decrease to a steady state value equivalent to the DC limiting current density.

The scientific basis for the previous paragraph is provided by work published by Ibl and colleagues,^{17,18,19} where a “duplex diffusion layer,” consisting of an inner pulsating layer and an outer stationary layer was developed. Modeling work by Landolt has also suggested the existence of a pulsating diffusion layer.²⁰ Since the thickness of the pulsating diffusion layer is determined by the waveform parameters, we call this layer the “electrodynamic diffusion layer” (Fig. 2).²¹ By assuming a linear concentration gradient across the pulsating diffusion layer and conducting a mass balance, Ibl derived the pulsating diffusion layer thickness (δ_p) as:¹⁸

$$\delta_p = (2Dt_{\text{on}})^{1/2} \quad (4)$$

where D is the diffusion coefficient and t_{on} is the pulse length. When the pulse on-time is equal to the transition time (τ), the concentration of reacting species at the interface drops to zero precisely at the end of the pulse. An expression for τ is provided in the following equation:

$$\tau = [(nF)^2 C_b^2 D] / 2i_p^2 \quad (5)$$

More exact solutions are given by integrating Fick’s diffusion equation:

$$\delta_p = 2[(Dt_{\text{on}})/\pi]^{1/2} \quad (6)$$

$$\tau = \pi[(nF)^2 C_b^2 D] / 4i_p^2 \quad (7)$$

More recently, Yin,²² using a similar approach to Ibl’s, derived the same equation for the pulsating diffusion layer for “pulse-with-reverse” electrochemical processes. The ratio between the limit-

ing current density realized in the pulse/pulse reverse process, i_p , versus that in steady state, i_{lim} , is:

$$i_p/i_{\text{lim}} = [\delta_p/\delta (1 - \gamma_a) + \gamma_a]^{-1} \quad (8)$$

Since δ_p must be smaller than δ , higher instantaneous limiting current densities can be achieved in pulsed processes. The extent of this increase is based on the δ_p/δ ratio, which is directly influenced by the anodic pulse on-time. A higher limiting current density relates directly to a higher instantaneous metal removal rate. Therefore, the overall removal rate of a pulsed process can rival that of a DC process despite a duty cycle that is less than 100%, while enjoying enhanced process performance.

Another key consideration when trying to design a waveform for a particular finishing environment is the current distribution that will develop. There are two important aspects that must be taken into account. First, is the current distribution a function of primary (geometrical), secondary (kinetic) or tertiary (mass transport) considerations? Second, what is the relationship between the pulsating boundary layer thickness and the surface profile height?

First, the current distribution developed in constant current processes is controlled by primary effects. Through the application of pulsed electric fields, the pulse/pulse reverse process supplements the primary effects with both secondary and tertiary effects. The addition of these effects tends to make the current distribution more uniform, as compared to primary current distribution alone. Therefore, the current distribution in the pulse/pulse reverse process can be substantially different than that achieved in conventional constant current processes. By understanding the influence of the pulse waveform parameters on current distribution, parameters can be selected to enhance either localized current distribution (for surface leveling or edge deburring) or uniform current distribution (for surface polishing).

If the waveform is selected such that the pulse on-time is much longer than the transition time, tertiary effects play a dominant role in the current distribution. For this case, additional criteria that influence current distribution are the concepts of macroprofile and microprofile. In a macroprofile (Fig. 3, left), the roughness of the surface is large compared with the thickness of the diffusion layer, and the diffusion layer tends to follow the surface contour. Under mass transport or diffusion control, a macroprofile results in a uniform current distribution and conformal dissolution. In a

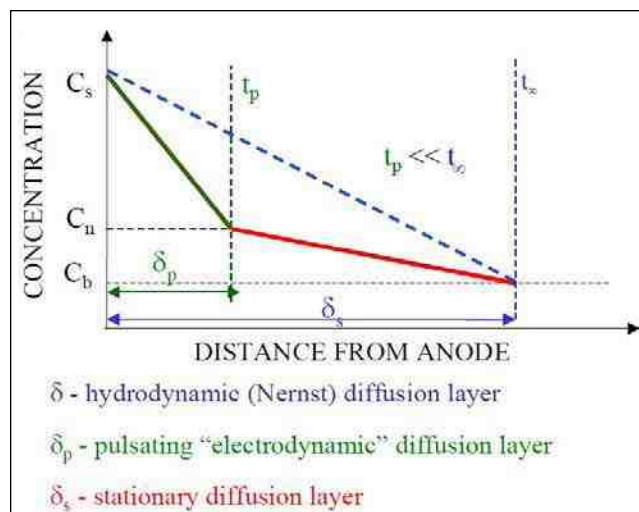


Figure 2—Schematic representation of the duplex diffusion layer.

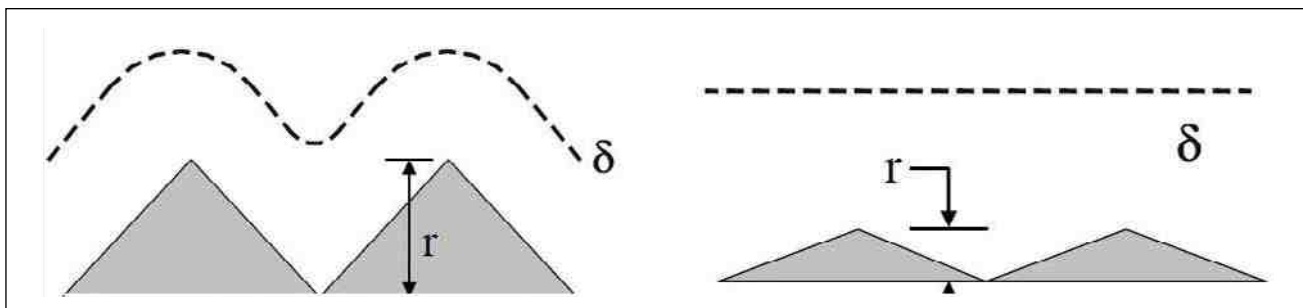


Figure 3—Left: macroprofile ($\delta \sim r$); right: microprofile ($\delta > r$).

microprofile (Fig. 3, right), the roughness of the surface is small compared with the thickness of the diffusion layer. Under mass transport or diffusion control, a microprofile results in a localized current distribution and non-uniform dissolution. Note that in the absence of mass transport control, the primary and/or secondary current distribution effects control the process.

Waveform sequencing

Our experience has also shown the need for waveform sequencing (Fig. 4) when polishing surfaces to a very low R_a . Depending on the flow rate of electrolyte past the surface, a macroprofile may initially exist, and a specific waveform is chosen to polish this surface. As the surface is polished and becomes much smoother, the macroprofile may transition to a microprofile. In order for further polishing (lower R_a) to be achieved, the waveform must be changed. An advantage of the pulse/pulse reverse process is that these distinct waveforms may be preprogrammed into the rectifier, so that process control is simplified. We have used this approach to electropolish stainless steel valves to an R_a of 0.12 μm for a customer application.

Experimental procedure

Sample preparation

Niobium foil, 99.9% pure,** was purchased (Fig. 5) and cut into same size coupons for the electropolishing studies. Final coupon sizes had the following dimensions: 25.4 mm \times 25.4 mm \times 3 mm (Fig. 6). Since a high precision cut was needed, wire electrical discharge machining (WEDM) was employed. As WEDM is an electrothermal process, there was formation of an oxide layer on the sample being cut. As can be observed in Fig. 6, the niobium coupon after WEDM was darker as compared to the stock material shown in Fig. 5. Therefore, mechanical polishing was employed in order to remove the oxide layers and obtain a standardized surface finish before the electropolishing experiments.

** Goodfellow Corporation, Oakdale, PA.

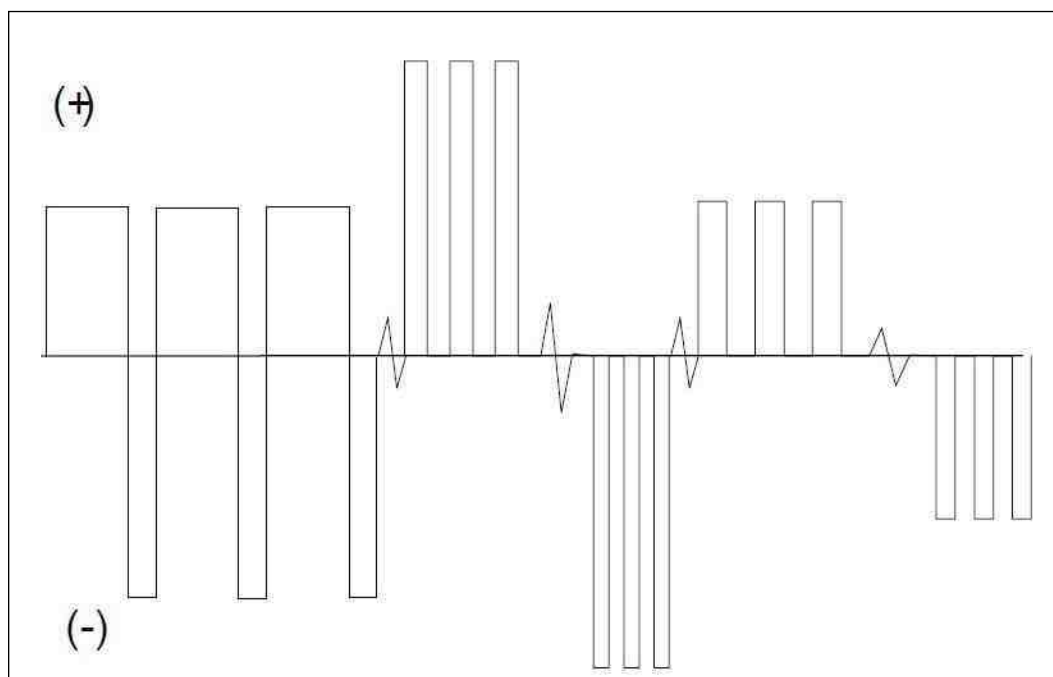


Figure 4—Generic waveform sequencing, used to electropolish materials to a very low R_a .



Figure 5—15 cm × 15 cm × 0.3 cm Nb foil, 99.9% pure.

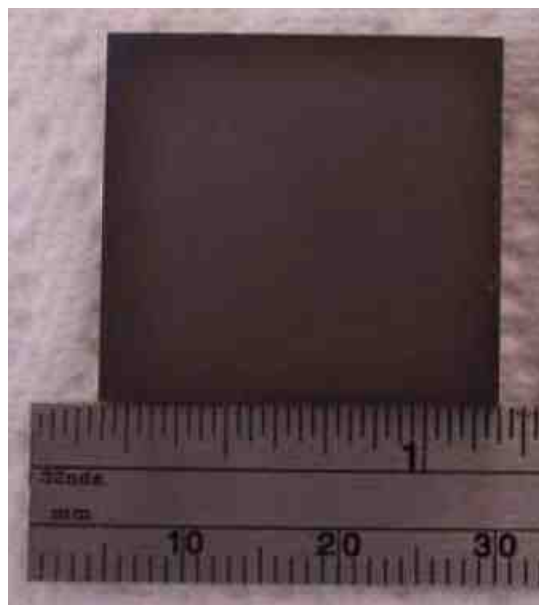


Figure 6—25 mm × 25 mm × 3 mm Nb coupon after WEDM.

Electrochemical cell

Figure 7 shows the photograph (left) and an AutoCAD drawing (right) of a low flow channel cell that accommodates the 25.4 mm × 25.4 mm × 3 mm niobium coupons. This cell allowed the study of electropolishing niobium at different cathode-to-anode distances, as well as different electrolyte velocities. The flexibility inherent within this cell design enabled an investigation of the effect of primary current distribution in conjunction with the pulse/pulse reverse process for electropolishing niobium.

The 25.4 mm × 25.4 mm × 3 mm coupons were mechanically polished using 60-grit or 180-grit silicon carbide (SiC) grinding paper, giving an initial R_a of approximately 1.53 μm or 0.56 μm , respectively. The niobium coupons were cleaned ultrasonically using a Branson ultrasonic cleaner (Model 3510) in 5% NaOH and DI water. Only an area of 12.7 mm × 12.7 mm of the niobium coupon was used for DC polarization studies and electropolishing experiments. The rest of the area was masked with plating tape to avoid edge effects.

Electrolyte selection

Development of the pulse/pulse reverse process typically begins with a polarization curve study, which is a plot of the anode voltage, E_a , as a function of anodic current density, i_a , and provides information on active and passive regions of materials in different electrolytes.²³ Generic polarization curves, shown in Fig. 8, illustrate the anodic behavior of a metal in various electrolytes. Curve 1 shows the behavior of a metal in an active electrolyte (such as NaCl), and Curve 2 shows the behavior of a metal in a passive electrolyte (such as Na_2SO_4). Before the electric field is applied, the metal anode immersed in the electrolyte has a steady-state voltage (E_{ss}). When the power is applied, the electrode voltage will shift in the positive direction from E_{ss} to E_{ab} (the breakdown voltage). Above E_{ab} , the current density rises abruptly due to the dissolution reactions occurring on the anode (region AB). The dissolution rate of the anode metal stops increasing when a limiting current density i_{lim} is reached (BC region), where the metal atoms form metal

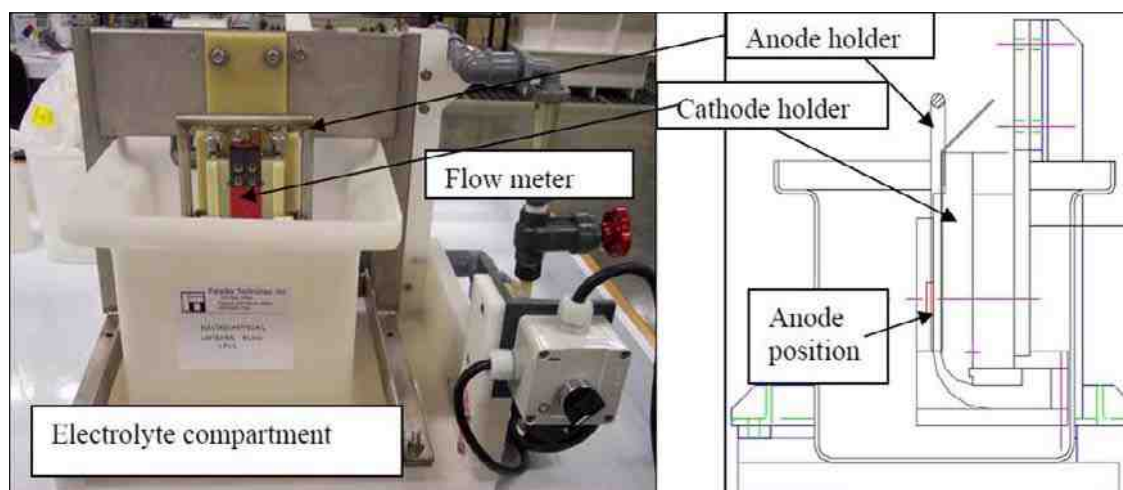


Figure 7—Photograph (left) and side view AutoCAD drawing (right) of the low flow channel cell used to electropolish 25.4 mm × 25.4 mm × 3 mm Nb coupons.

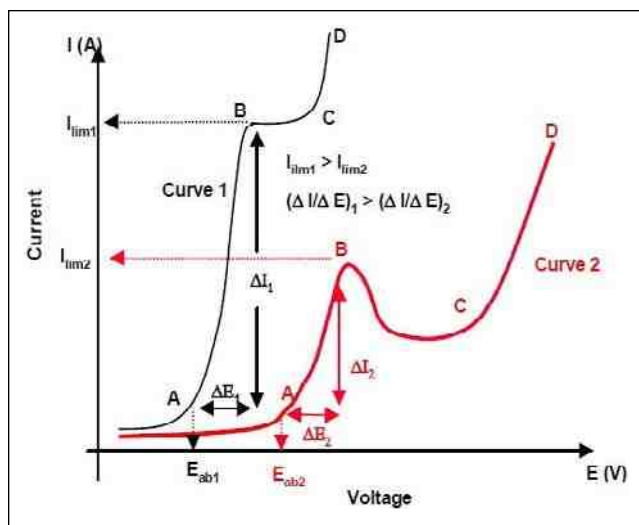


Figure 8—Typical polarization curves for metal in different electrolytes.

ions and compounds with the activating anions and pass into the electrolyte. The limiting current density i_{lim} and the ratio of ΔI to ΔE (the slope of AB on the polarization curve) can be defined as the metal dissolution rate and current efficiency in the electrolyte, respectively.

DC polarization studies were carried out in order to select an electrolyte that would enable the process for electropolishing niobium coupons. The two-electrode DC polarization studies were performed on 25.4 mm × 25.4 mm × 3 mm niobium coupons to study the electrochemical activity (*e.g.*, total current density) of niobium in different electrolyte type and concentrations. A platinum-coated niobium mesh was used as the cathode. All polarization curve experiments were performed at room temperature (~20°C). A TecNu power supply was used for this study (Model SPR-300/100/48-3). The cell voltage was raised by increments of five volts per minute. Total current densities were read from the oscilloscope trace recorded on a FLUKE 196C Scopemeter color system.

Results and discussion

Polarization curve study

Figure 9 summarizes the electrochemical activity of niobium substrates in different electrolytes, low and high concentrations of sodium chloride (NaCl), sulfuric acid (H₂SO₄), sodium bromide (NaBr), sodium fluoride (NaF) and phosphoric acid (H₃PO₄). In all cases, no breakdown of the niobium was observed. Any current measured is assumed to be associated with water oxidation ($2H_2O \rightarrow O_2 + 2H^+ + 2e^-$) and niobium anodization. The highest and lowest total current density observed for voltages up to 70 V was in the H₂SO₄ and NaF electrolytes, respectively.

This data demonstrates the tenacity of the niobium oxide film. DC polarization studies were unable to shed any light on the conditions that would be required to break down the oxide film without the use of hydrofluoric acid. Therefore, based on our prior experience in surface finishing of passive materials, we chose to develop electrochemical waveforms to electropolish niobium. Historically, we have combined the waveforms with process parameters such as cell geometry and uniform hydrodynamic conditions

for successful metal removal of passive metal and alloys.^{13,24} An advantage of electrolyte flow is the removal of undesired byproducts from the surface of the substrate being electropolished, such as niobium ions, heat and bubbles (resulting mainly due to oxygen and hydrogen generation from water electrolysis).

Electropolishing of niobium

In the initial experiments, the constant parameters were electrolyte velocity = 0.4 m/sec, run time = 10 min, forward (V_f) and reverse voltage (V_r), anode-to-cathode distance = 5 mm, and ambient temperature (~20°C). Since the electrochemical cell did not have temperature control built in, the electrolyte temperature rose from an initial value of 20°C to around 27°C by the end of every experiment. A design of experiments set was performed using MINITAB®. Two different frequencies were used at two different forward duty cycles (D_f) (Table 1).

Figure 10 shows representative niobium coupons after electropolishing experiments were attempted in a H₂SO₄ electrolyte using the pulse/pulse reverse waveforms in Table 1. Run #1 (Fig. 10-left) showed no evidence of etching. The different colors observed represent niobium oxide layers formed on the substrate. Run #2 (Fig. 10-center) showed some degree of etching, which suggested that niobium substrates could be uniformly electrochemically etched in an electrolyte free of HF. Run #4 (Fig. 10-right) also showed some degree of etching, but much lower as compared to Run #2.

Based on these preliminary results, the pulse/pulse reverse waveform used for Run #2 was further explored. Specifically, Run #5 used the same waveform parameters as Run #2, but the coupon was electropolished for 37 min instead of 10 min. The resulting niobium coupon surface is shown in Fig. 11. A thickness of 100 μm of niobium was successfully removed uniformly from the coupon at an average removal rate of 2.7 μm/min over an area of approximately 161 mm².

Having achieved uniform removal of niobium in an HF-free electrolyte, the next step was to optimize the electropolishing process to achieve surface roughness similar or better to the ones obtained by state-of-the-art electropolishing techniques (*e.g.*, around 0.1 to 0.2 μm). The following process and cell parameters were studied:

- Effect of applied peak voltage
- Effect of polishing time
- Effect of anode-to-cathode distance
- Effect of electrolyte flow velocity

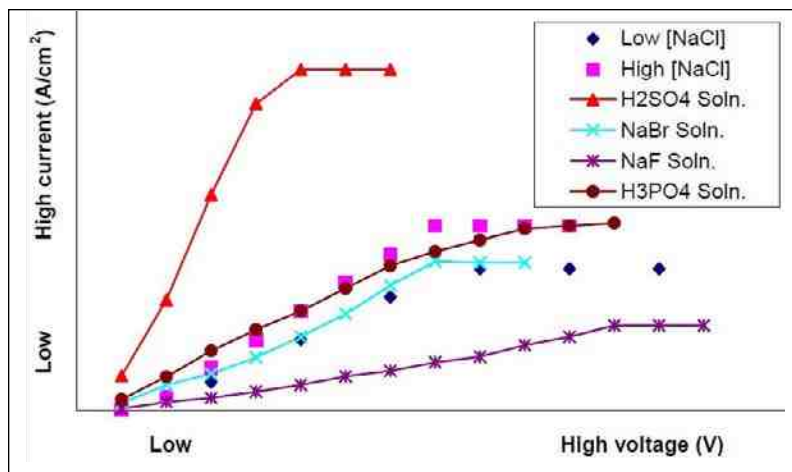


Figure 9—Two-electrode polarization curves of Nb in different electrolytes.

Table 1

Design of experiments using pulse/pulse reverse waveforms to electropolish Nb in a H_2SO_4 electrolyte for 10 min and an anode-cathode distance of 5 mm

Run No.	Waveform No.	Frequency	Forward (Anodic) Duty Cycle, %	V_f	V_r
1	PRC1	Low	High	Low	Constant
2	PRC2	High	Low	Low	Constant
3	PRC3	Low	Low	Low	Constant
4	PRC4	High	High	Low	Constant

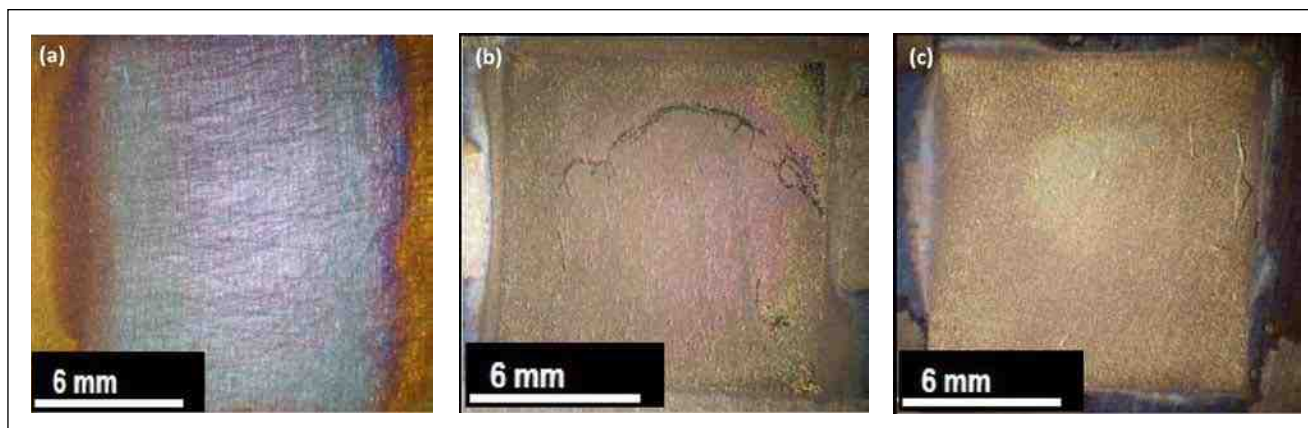


Figure 10—Representative Nb coupons after electropolishing experiments at ambient temperature ($\sim 20^\circ C$) in H_2SO_4 electrolytes using their respective pulse/pulse reverse waveforms listed in Table 1.

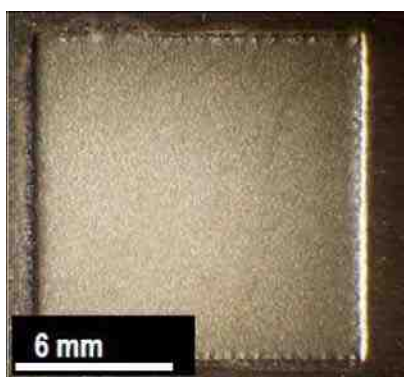


Figure 11—Nb coupon of Run #5 after electrochemical polishing at $2.7 \mu m/min$ in a H_2SO_4 electrolyte.

Effect of peak voltage on niobium electropolishing

The effect of raising V_f in PRC2 (V_f = low potential) on niobium electropolishing performance was studied. Two higher forward voltages were explored, PRC5 (V_f = intermediate potential) and PRC6 (V_f = high potential). In both cases, the other pulse/pulse reverse process parameters, frequency, D_f and V_r were kept the same as for waveform PRC2.

Figure 12 shows niobium coupons of Runs #5 (PRC2), #6 (PRC5) and #7 (PRC6), after electropolishing in a H_2SO_4 electrolyte, varying V_f . Figure 13 summarizes the effect of peak voltage on niobium surface finish. The roughest surface finish was

obtained using PRC2. When V_f was increased in PRC5, the surface finish R_a of niobium dropped from $1.38 \mu m$ to $0.29 \mu m$. When PRC6 was used, the niobium surface finish started getting rougher again and surface discoloration was observed. Therefore, for future experiments during this work, we used waveform PRC5.

Effect of electropolishing time on niobium surface roughness, R_a

Once a set of process parameters for polishing niobium in H_2SO_4 had been determined, the next phase of study was aimed at minimizing unnecessary polishing time. The optimum waveform (to date) developed previously (PRC5) was applied to a niobium coupon in 10-min steps. After each 10-min step, the coupon was removed from the cell, rinsed with DI water and dried with compressed air, and the R_a was measured. The coupon was then returned to the electrochemical cell for a further 10 min of electropolishing.

Figure 14 shows the effect of electropolishing time on the average surface roughness of a niobium coupon using waveform PRC5. The surface finish decreased slowly with time until 30 min of polishing had been applied, and then there was a more rapid decrease in R_a down to $0.2 \mu m$ between 30 and 50 min. After 50 min, further decreases in R_a were not observed. This result suggests the need for waveform sequencing, as briefly discussed in the Introduction section, to further decrease the niobium surface roughness.

During electropolishing, the material removal rate was constant, at approximately $5.0 \mu m/min$, about ten times faster than conventional electropolishing techniques that use HF.

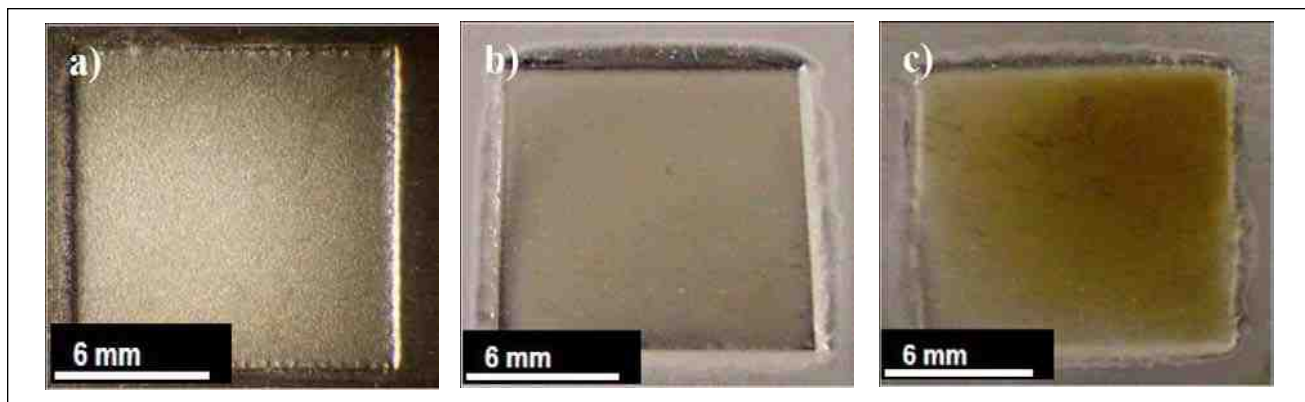


Figure 12—Nb coupons after electropolishing in a H_2SO_4 electrolyte at room temperature ($\sim 20^\circ C$) at varying V_f : (a) Run #5 (PRC2); (b) Run #6 (PRC5) and (c) Run #7 (PRC6).

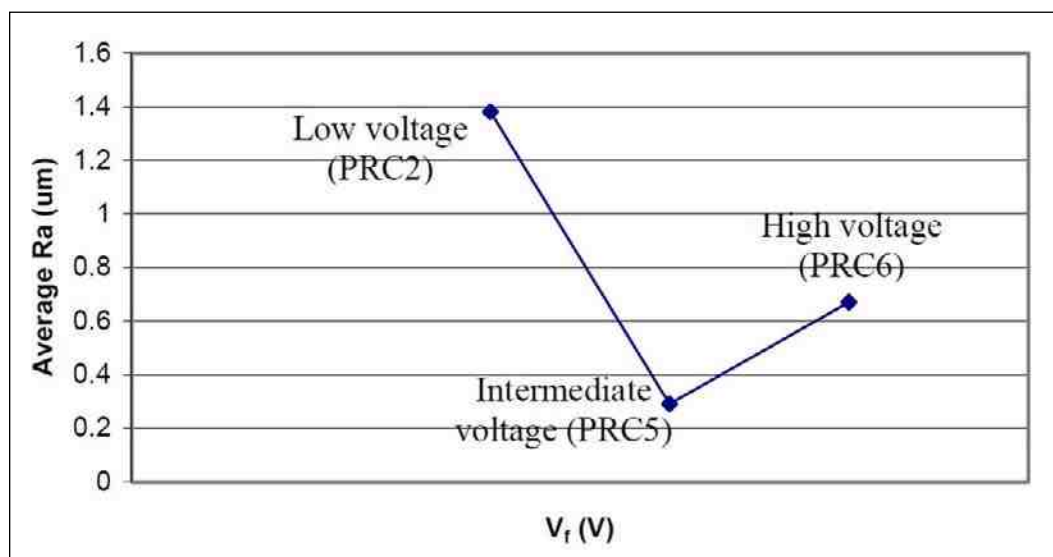


Figure 13—Effect of V_f on the average surface roughness of Nb after electropolishing in H_2SO_4 electrolytes at ambient temperature ($\sim 20^\circ C$); Run #5 (PRC2), Run #6 (PRC5) and Run #7 (PRC6).

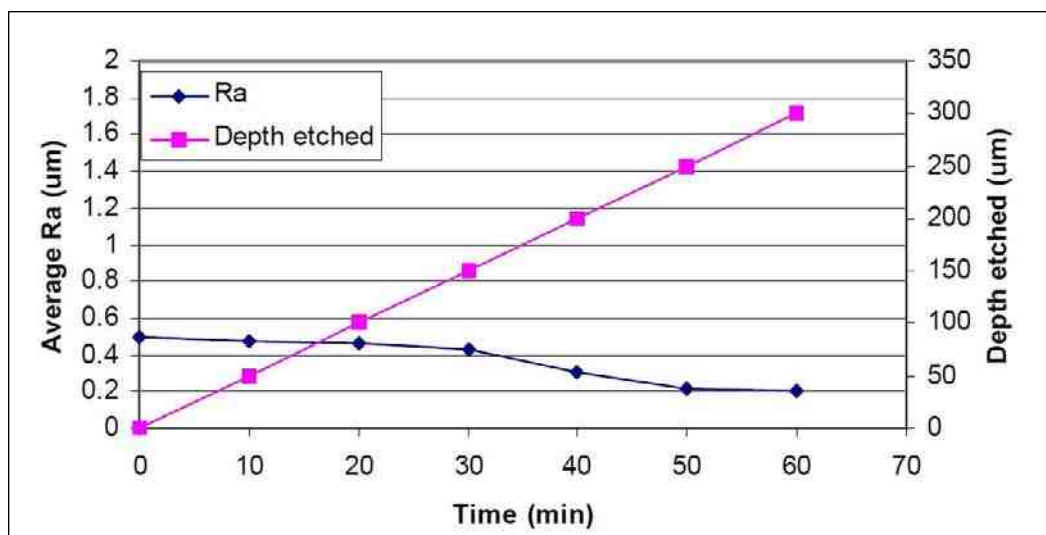


Figure 14—Effect of time on the average surface roughness of Nb after electropolishing in a H_2SO_4 electrolyte at ambient temperature ($\sim 20^\circ C$), using waveform PRC5, and $R_{ao} = 0.56 \mu m$ (Run #8).

The effect of the niobium initial surface roughness, R_{ao} , on the final surface roughness, R_{af} , was also studied by performing electropolishing time studies at different R_{ao} values. Figure 15 compares the effect of time on the average surface roughness of a niobium coupon after electropolishing in a H_2SO_4 electrolyte for $R_{ao} = 0.56 \mu m$ (Run #8) and $R_{ao} = 1.53 \mu m$ (Run #9). For the higher initial surface roughness, there was a significant decrease in R_a after 10 min, from $1.53 \mu m$ to $\sim 0.85 \mu m$. Thereafter, R_a was decreased further by increasing the electropolishing time up to 60 min down to an R_{af} value of $0.33 \mu m$. Further decreases in surface finish did not occur after 50 min, again suggesting the need for waveform sequencing to obtain a lower R_a .

Effect of varying cell parameters on the R_a of electropolished niobium

The effects of anode-cathode distance as well as electrolyte velocity on the surface roughness of electropolished niobium were studied. The effect of anode-cathode distance and electrolyte velocity

on niobium surface finish was studied using waveform PRC5 at ambient temperature ($\sim 20^\circ C$). Each experiment ran for 40 min in a H_2SO_4 electrolyte.

Effect of anode-to-cathode distance on R_a : The results of the anode-to-cathode distance study are summarized in Fig. 16. For anode-to-cathode distances up to 10 mm, R_a decreased to a minimum value of $0.15 \mu m$. At anode-to-cathode distances greater than 10 mm, R_a increased with anode-to-cathode distance, becoming almost flat at distances larger than 25 mm. After the anode-to-cathode distance study, all subsequent experiments were performed with the cell geometry at which an R_a value of $0.15 \mu m$ was obtained (an anode-to-cathode distance of 10 mm).

Effect of electrolyte velocity on R_a : The effect of electrolyte velocity was another important variable that was studied to understand its effect on niobium electropolishing. In these experiments, the anode-to-cathode distance used was 10 mm. The results are summarized in Fig. 17. Three different electrolyte velocities were

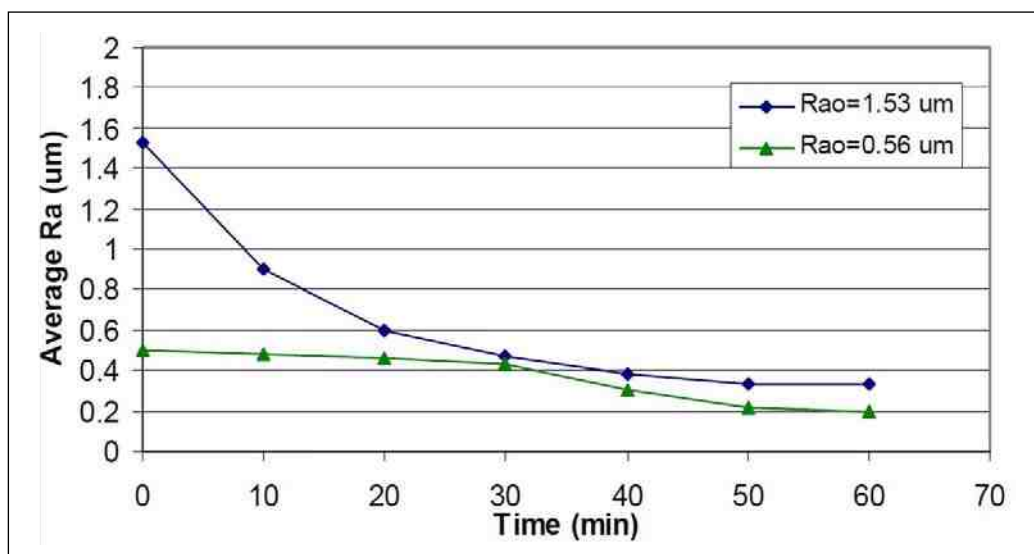


Figure 15—Effect of time on the average surface roughness of Nb after electropolishing in H_2SO_4 electrolytes at room temperature ($\sim 20^\circ C$) using waveform PRC5 and different R_{ao} values.

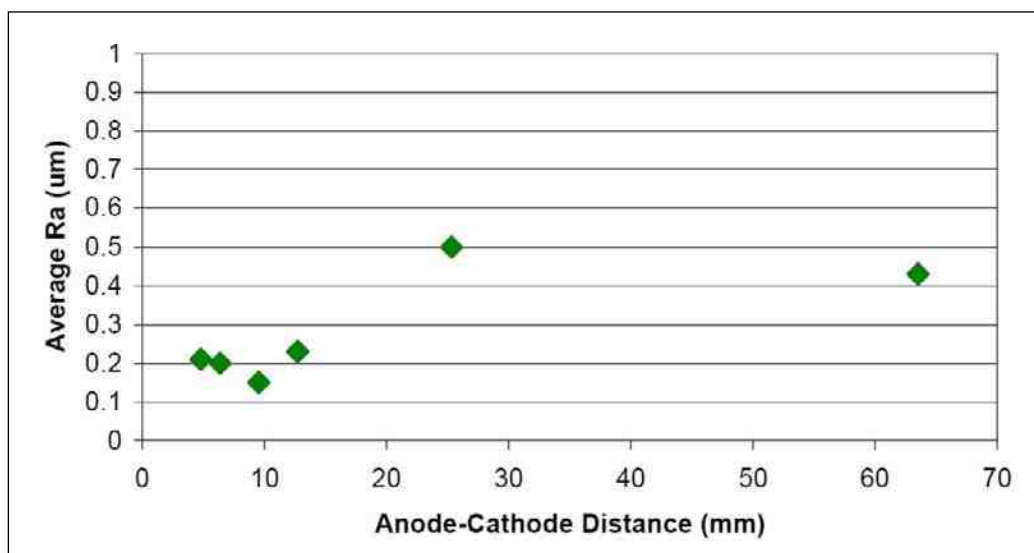


Figure 16—Effect of anode-to-cathode distance on the average surface roughness of Nb after electropolishing in a H_2SO_4 electrolyte at ambient temperature ($\sim 20^\circ C$), using waveform PRC5. Experiments correspond to Runs #10 through #15 in order.

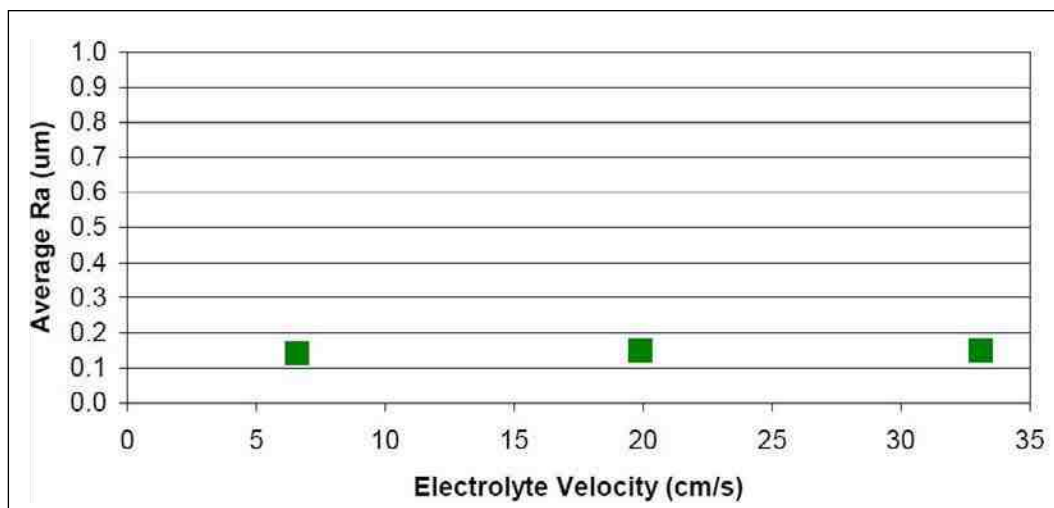


Figure 17—Effect of electrolyte velocity on the average surface roughness of Nb after electropolishing in a H_2SO_4 electrolyte at ambient temperature ($\sim 20^\circ C$), using waveform PRC5 and an anode-to-cathode distance of 10 mm.

explored, 33.1 cm/sec (Run #16), 19.9 cm/sec (Run #17) and 6.6 cm/sec (Run #18). The final R_a values were 0.14, 0.15 and 0.15 μm , respectively. The photographs of bright and smooth polished niobium substrates corresponding to each run are shown in Fig. 18. There did not appear to be a significant effect of electrolyte velocity when electropolishing niobium in this cell configuration. However, the results of an experiment with an electrolyte velocity of 0 cm/sec (Run #19), suggested that there must be some degree of agitation in order to achieve uniform, smooth polishing of the niobium surface.

Characterization of electropolished niobium substrates

Effect of profilometer scan length on R_a : The effect of the profilometer scan length on the average surface roughness, R_a , was studied. Figure 19 shows the effect of scan range on the R_a value of niobium after electropolishing in H_2SO_4 electrolytes using waveform PRC5 at different electrolyte velocities. Two different scan lengths, 1.25 mm and 4 mm, were used on the same area of the electropolished niobium coupons. The effect of scan range on R_a was almost identical for the three different electrolyte velocities. R_a increased slightly from around 0.1 μm to 0.15 μm by increasing the scan length from 1.25 mm to 4.0 mm. This data suggests that the macroscale surface roughness is slightly higher than the microscale roughness.

Scanning electron microscopy evaluation: Figure 20 (left) shows an SEM micrograph of the surface morphology of a niobium substrate electropolished using a H_2SO_4 electrolyte, waveform PRC5 at a velocity of 6.6 cm/sec and anode-to-cathode distance of 10 mm. The image confirms that a smooth surface of niobium can be obtained, not only at a macroscale, but also at a microscale finish using the pulse/pulse reverse process in an electrolyte free of HF.

Energy Dispersive Spectroscopy (EDS) was used to analyze the surface of electropolished niobium coupons. Figure 20 (right) shows an EDS spectrum of the elements detected on the surface of the analyzed area on the niobium substrate. The spectrum was mainly dominated by the presence of niobium. Dr. Allen G. Jackson, Program Manager of the Department of Mechanical & Materials Engineering at Wright State University, who performed the SEM and EDS analysis, believes that even though oxygen is present in very small amounts (he estimates about 0.5 wt%), its peak is too small to be statistically significant. In such a case, the small amounts of oxygen would correspond to a very thin layer of Nb_2O_5 (about 5 nm thick) that forms naturally on niobium. The elements and their respective weight percentages are listed in Table 2. There was no evidence of impurities present on the niobium surface using EDS analysis.

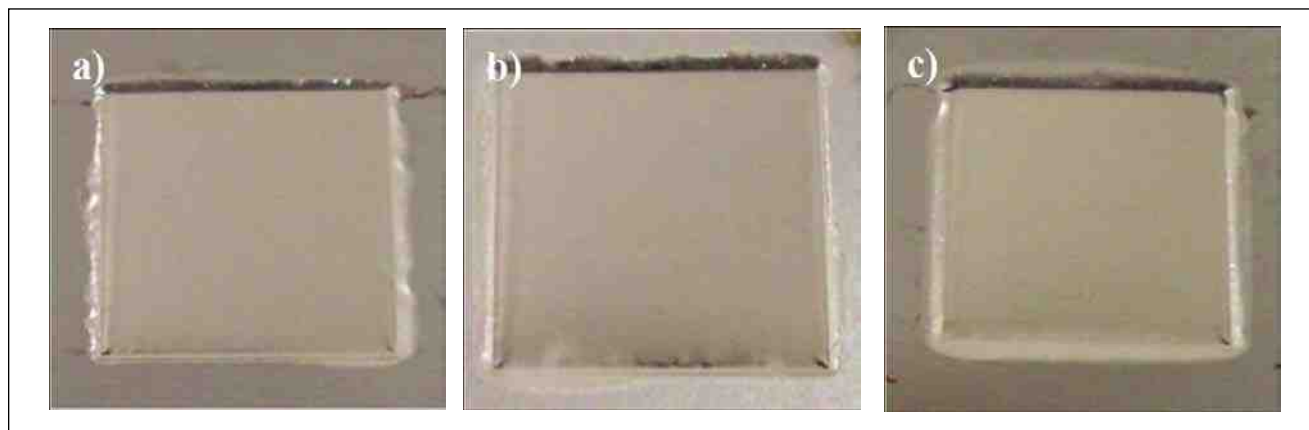


Figure 18—Photographs of Nb coupons after electropolishing in H_2SO_4 electrolytes at room temperature ($\sim 20^\circ C$), using waveform PRC5, an anode-to-cathode distance of 10 mm and varying the electrolyte velocity: (a) 6.6 cm/sec, (b) 19.9 cm/sec and (c) 33.1 cm/sec.

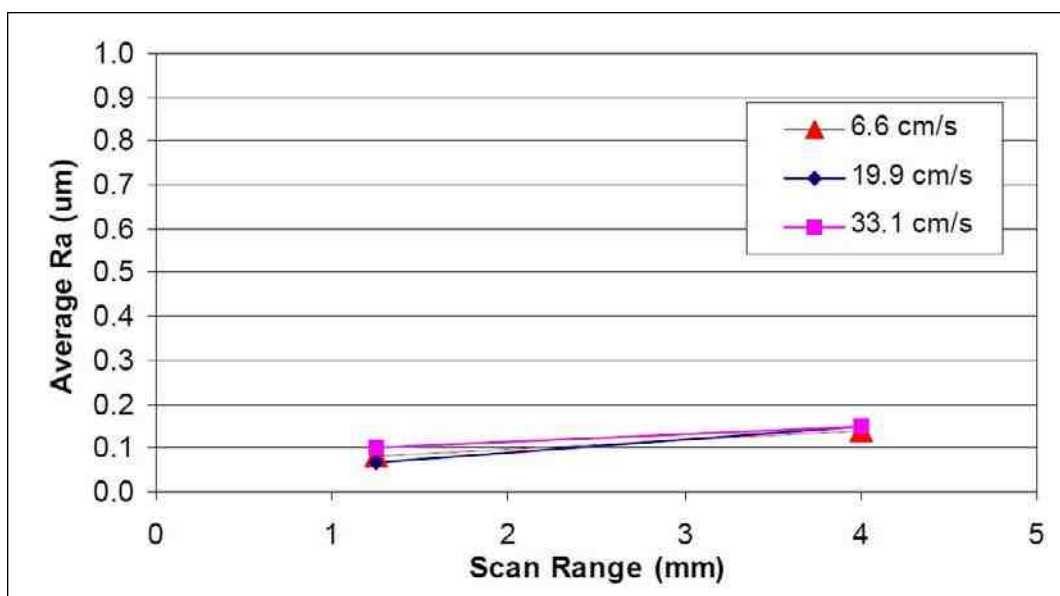


Figure 19—Effect of scan range on the average surface roughness of Nb after electropolishing in H_2SO_4 electrolytes, using waveform PRC5 and different electrolyte velocities.

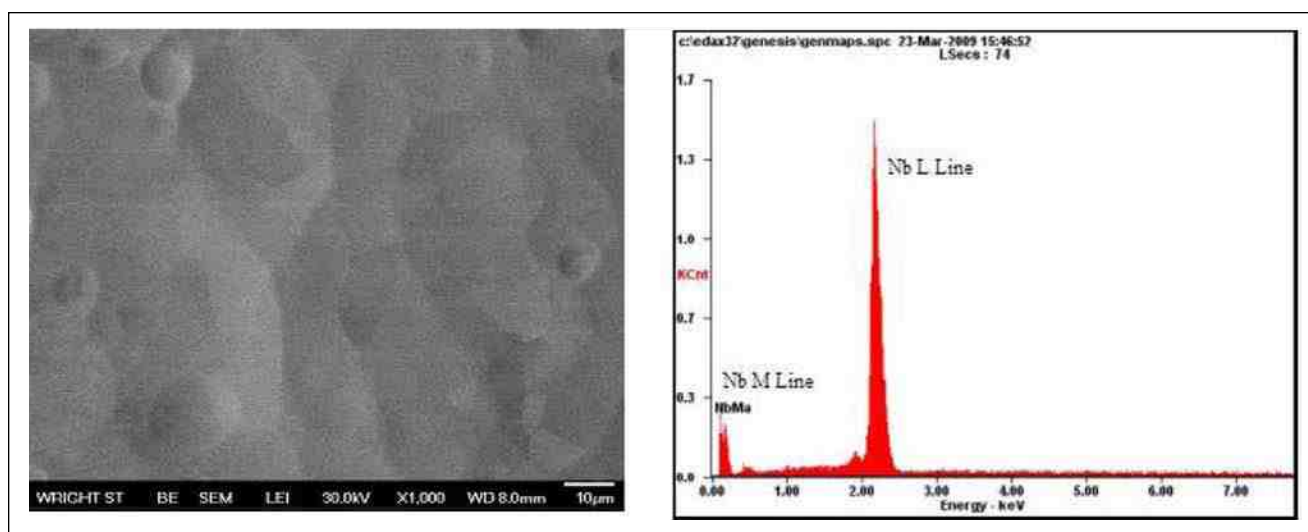


Figure 20—SEM micrograph (left) and EDS of a Nb substrate after electropolishing in H_2SO_4 electrolytes at room temperature ($\sim 20^\circ C$), using waveform PRC5, an anode-to-cathode distance of 10 mm and an electrolyte velocity of 6.6 cm/sec.

Table 2

List of elements and wt% detected using EDS on Nb substrates after electropolishing in H_2SO_4 electrolytes at room temperature ($\sim 20^\circ C$), using waveform PRC5, an anode-to-cathode distance of 10 mm and an electrolyte velocity of 6.6 cm/sec

Element	Weight %	Atomic %
Niobium (Nb)	99.5	97.2
Oxygen (O)	0.5	2.8

Summary of results

Table 3 compares the pulse/pulse reverse electropolishing process with chemical polishing and conventional electropolishing, state-of-the-art techniques employed to polish superconducting radio frequency accelerators made of niobium. Unlike chemical and conventional electropolishing, the pulse/pulse reverse process does not use hydrofluoric acid, achieving electropolishing rates up to five to ten times faster, respectively. Surface roughness values average of about one order of magnitude lower than obtained by chemical polishing.

Conclusions

The overall objective of this work was to demonstrate the technical and economic feasibility of the pulse/pulse reverse process for polishing niobium for superconducting radio frequency cavities in an environmentally benign electrolyte. Results indicated that

Table 3

Summary table comparing chemical polishing, conventional electropolishing and pulse/pulse reverse electropolishing

	Chemical polishing	Conventional electrochemical polishing	Pulse/pulse reverse electropolishing
Electrolyte	HF/HNO ₃ /H ₃ PO ₄ (1:1:3)	HF (10%): H ₂ SO ₄ (90%)	H ₂ SO ₄
Hydrofluoric acid	Yes	Yes	No
Etch rate, $\mu\text{m}/\text{min}$	1.0	0.5	5.0
R_a , μm	1.0	0.1	0.1
Temperature, $^{\circ}\text{C}$	15 (Chilled)	30-35 (Chilled)	20

the pulse/pulse reverse process could (a) uniformly electropolish niobium to a microscale finish (0.1 μm) in a hydrofluoric acid-free electrolyte and (b) increase electropolishing rates about 10 times faster than state-of-the-art techniques that use hydrofluoric acid. In addition, SEM/EDS analysis showed that electropolished niobium surfaces free from contamination were obtained.

The results/attributes just mentioned, make the pulse/pulse reverse HF-free electropolishing process an ideal polishing technique not only for niobium cavities, but also for surgical devices and metallic implants made of niobium, titanium, titanium-nickel and stainless steel alloys. The process is anticipated to be cost effective compared to conventional polishing methods due to the robust control mechanisms and minimal associated waste.

Acknowledgement

This material is based upon work supported by the Department of Energy under Award Number DE-FG02-08ER85053.

Disclaimer

This report was prepared as an account of work sponsored by an agency of the United States Government. Neither the United States Government nor any agency thereof, nor any of their employees, makes any warranty, express or implied, or assumes any legal liability or responsibility for the accuracy, completeness, or usefulness of any information, apparatus, product, or process disclosed, or represents that its use would not infringe privately owned rights. Reference herein to any specific commercial product, process, or service by trade name, trademark, manufacturer, or otherwise does not necessarily constitute or imply its endorsement, recommendation, or favoring by the United States Government or any agency thereof. The views and opinions of authors expressed herein do not necessarily state or reflect those of the United States Government or any agency thereof.

References

1. K. Saito, *Proceedings of the 2003 Particle Accelerator Conference*, p. 462 (2003); <http://accelconf.web.cern.ch/accelconf/p03/PAPERS/ROAA002.pdf> (last accessed 09/14/09).
2. Anon., "Argonne-Fermilab BCP System Coming Together," ILC Newsline (4 January 2007); http://www.linearcollider.org/newsline/archive/2007/20070104_feature1.pdf (last accessed 09/14/09).
3. A. T. Wu, *et al.*, *Applied Surface Science*, **253** (6), 3041 (2007).
4. L. Lilje, *et al.*, *Nuclear Instruments and Methods in Physics Research A*, **524** (1-3), 1 (2004).
5. I. Mickova, *et al.*, *Croatica Chemica Acta*, **79** (4), 527 (2006); http://hrcaak.srce.hr/index.php?show=clanak&id_clanak_jezik=8911; link to full text (last accessed 09/14/09).
6. L. D. Zardiackas, M. J. Kraay & H. L. Freese, *Titanium, Niobium, Zirconium, and Tantalum for Medical and Surgical Applications*, ASTM International, Materials Park, OH, 2006; p. 268.
7. L. Jiin-huey Chern, J. Chien-ping & L. Chih-min, U.S. Patent 6,752,882 (2004).
8. Personal communication, Prof. Lyle Zardiackas, April 8th, 2009.
9. N. Eliaz & O. Nissan, *J. Biomedical Materials Research - Part A*, **83A** (2), 546 (2007).
10. J.W. Dini, *Electrodeposition-The Materials Science of Coatings and Substrates*, Noyes Publications, Park Ridge, NJ, 1993; Chapter 7, p. 56.
11. J-C. Puipe & F. Leaman, *Theory and Practice of Pulse Plating*, NASF, Washington, DC, 1986.
12. J.J. Sun, *et al.*, *Plating & Surface Finishing*, **89** (5), 94 (2002).
13. A. Lozano-Morales, *et al.*, *J. Appl. Surf. Finish.*, **2** (3), 192 (2007).
14. H.Y. Cheh, *J. Electrochem. Soc.*, **118**, 551 (1971).
15. H.Y. Cheh, *J. Electrochem. Soc.*, **118**, 1132 (1971).
16. K. Viswanathan, M.A. Farrell-Epstein & H.Y. Cheh, *J. Electrochem. Soc.*, **125**, 1772 (1978).
17. N. Ibl, J. C. Puipe & H. Angerer, *Surface Technology*, **6** (4), 287 (1978).
18. N. Ibl, *Surface Technology*, **10** (2), 81 (1980).
19. N. Ibl, *Proc. 2nd International Pulse Plating Symposium*, NASF, Washington, DC, 1981.
20. D. Landolt, in *Theory and Practice of Pulse Plating*, J-C. Puipe & F. Leaman, Eds., NASF, Washington, DC, 1986.
21. E.J. Taylor, *et al.*, *Proc. AESF SUR/FIN 2001*, NASF, Washington, DC, 2001; p. 504; also in *Plating & Surface Finishing*, **89** (5), 88 (2002).
22. K-M. Yin, *Surface and Coatings Technology*, **88** (1-3), 162 (1996).
23. E. Rumyantsev & A. Davydov, *Electrochemical Machining of Metals*, MIR Publishers, Moscow, 1989.
24. J.J. Sun, E. J. Taylor & R. Srinivasan, *J. Materials Processing Technology*, **108** (3), 356 (2001).

About the authors



Dr. Alonso Lozano-Morales is a Project Engineer at Faraday Technology, Inc. He received his B.S. from Universidad de Sonora, Mexico and his Ph.D. degree from Louisiana State University, Baton Rouge, LA. All the above degrees are from the Department of Chemical Engineering. Currently, he is leading Faraday Technology's edge and surface finishing process technology development, as well as industrial coatings.



Dr. Maria E. Inman is the Research Manager at Faraday Technology Inc. She holds a B.E. in Metallurgical and Materials Engineering and a Ph.D. in Materials Engineering from the University of Auckland, New Zealand. Prior to joining Faraday Technology, she completed a two-year term as a post-doctoral research associate at the Center for Electrochemical Science and Engineering at the University of Virginia.



Dr. E. Jennings Taylor is the CEO and IP Director at Faraday Technology, Inc., Clayton, OH. He founded the company to develop and commercialize innovative electrochemical technology using sophisticated charge-modulated electric fields. The company's intellectual property has been successfully transferred both to government agencies and large manufacturers in the form of process engineering technology and products. He holds a B.A. in chemistry from Wittenberg University, an M.A. in technology strategy and policy from Boston University, and M.S. and Ph.D. degrees in materials science from the University of Virginia. He has published more than 70 technical papers and articles and holds many patents. He serves on the AESF Pulsed Electrodeposition Processes Committee and is Chairman of the Research Board.

Government Advisory Committee (GAC) Contributors

(as of 10/1/09)

\$1000 and Above

Gilbert & Jones, Inc.
Michael Dattilo, Seattle Puget Sound Branch
Gary A. Dybevik, Dave Hunter Company, Inc.
David G. Kelly, ASKO Processing, Inc.
Albert Walcutt, MPC Plating Inc.

\$500 and Above

American Electroplaters Society, Chicago Branch
Southwest United Industries
Walter Guns, Astro Industries Inc
Thomas Jensen, Jensen Plating Works, Inc
B. J. Mason, Mid-Atlantic Finishing Corp.
George H. Maze, American Nickeloid Co
Charles A. Remied, SERFILCO, Ltd.



\$100 and Above

Nayana S. Bora, CEF-4, Allied Finishing Inc
John T. Baker, Century Plating
William Furniss, Crown Plating Inc
Ken Hankinson, KCH Services, Inc.
Fred Hayduk, Luke Engineering & Mfg. Co.
Joanne Kiepora, CEF, Scientific Control Laboratories
Tom and Martha Martin
Billy J. Middleton, CEF-4, Industrial Metal Finishing, Inc.
John K. Murphy, Techmatic Inc.
Thomas A. Owens, Dyna-Plate Inc
Robert L. Reiten, Bend Plating Inc
William J. Saas, Coventya, Inc.
Victor M. Salazar, Omni Metal Finishing Inc
Naishadh K. Saraiya, CSL, Inc.
Stephen Schneider, John Schneider Assoc Inc
Robert P. Sica, New Brunswick Plating Inc
Milton F. Stevenson, Jr., CEF, Anoplate Corp
Joelie Zak, CEF-4, Scientific Control Labs Inc

\$10 and Above

David Calnan, Southern Water Treatment Company
Jack W. Dini
Gary Fennwald, ESC, 3M Company
Patricia J. Frisch, Amphenol Aerospace
Larry M. Frohnappel, Jan-Eze Plating Inc
James F. Laird, Allied-Signal Propulsion Engs
Mark E. Sano, L D McCauley/McGard Inc
Keith Sasaki